Inorg. Chem. **2004**, *43*, 4784–4786

$[NH_4]_2Mn_3(H_2O)_4[Mo(CN)_7]_2 \cdot 4H_2O$: Tuning Dimensionality and Ferrimagnetic Ordering Temperature by Cation Substitution

Xavier F. Le Goff,[†] Stéphanie Willemin,[‡] Claude Coulon,[†] Joulia Larionova,[‡] Bruno Donnadieu,[§] and Rodolphe Clérac*,[†]

Centre de Recherche Paul Pascal (CRPP), UPR CNRS 8641, 115 avenue du Dr. A. Schweitzer, 33600 Pessac, France, Laboratoire de Chimie Moléculaire et Organisation du Solide (LCMOS), UMR 5637, Université Montpellier II, Place E. Bataillon, 34095 Montpellier Cedex 5, France, and Laboratoire de Chimie de Coordination (LCC), UPR CNRS 8241, 31077 Toulouse, France

Received April 14, 2004

$[NH_4]_2Mn_3(H_2O)_4[Mo(CN)_7]_2 \cdot 4H_2O$ (**1**) has been synthesized by slow diffusion of aqueous solutions containing $K_4[Mo(CN)_7] \cdot 2H_2O$, $[Mn(H_2O)_6](NO_3)_2$, and $(NH_4)NO_3$. Compound **1** crystallizes in the monoclinic *C*2/*c* space group. The basic motif of the three-dimensional structure consists of a Mo1–Mn1 gridlike sheet parallel to the *bc* plane. Two of these sheets are connected through CN–Mn2–NC linkages to form a bilayer reminiscent of the $K_2Mn_3(H_2O)_6[Mo(CN)_7]_2 \cdot 6H_2O$ (**2**) two-dimensional structure. In **1**, $[NH_4]^+$ cations allow these bilayers to be connected through direct Mo1–CN–Mn1 bridges to form a three-dimensional network, whereas in **2**, they are isolated by $(H_2O)K^+$ cations. As shown by the magnetic measurements, this increase of dimensionality by counterion substitution induces an enhancement of the ferrimagnetic critical temperature from 39 K in **2** to 53 K in **1**.

In the past 20 years, the study of cyanide-based transition metal materials has been one of the major research trends in the field of molecule-based magnetism leading for example to room-temperature magnets,[1] photomagnetic properties,[2] high-spin molecules,[3] or single-molecule magnets.[4] Most of these remarkable physical properties have been obtained for materials incorporating $[M(CN)_6]$ building blocks, but curiously hepta-cyanometalate precursors have aroused less interest. Nevertheless, studies of the $[Mo^{III}(CN)_7]^{4-}/Mn^{II}$ system have led to few compounds that all order ferrimagnetically between 39 and 106 K.[5−10] Extending this family of materials, we report here the synthesis, crystal structure, and magnetic properties of $[NH_4]_2Mn_3(H_2O)_4[Mo(CN)_7]_2 \cdot 4H_2O$ (**1**), a new three-dimensional cyano-bridged ferrimagnet built from the $[Mo^{III}(CN)_7]^{4-}$ building block. This compound illustrates how counterions can control the structural dimensionality and, consequently, magnetic properties.

Under argon atmosphere, the slow diffusion in an H-shape tube of two aqueous solutions containing $K_4[Mo(CN)_7] \cdot 2H_2O$,[11] and $[Mn(H_2O)_6](NO_3)_2$ in the presence of $(NH_4)NO_3$, leads to dark green parallelepiped single crystals.[12] Single-crystal X-ray diffraction studies revealed that **1** crystallizes in the *C*2/*c* monoclinic space group with a three-

* To whom correspondence should be addressed. E-mail: clerac@crpp-bordeaux.cnrs.fr. Fax: (33) 5 56 84 56 00.

† CRPP.

‡ LCMOS.

§ LCC.

(1) Ferlay, S.; Mallah, T.; Ouahès, R.; Veillet, P.; Verdaguer, M. *Nature* **1995**, *378*, 701. Holmes, S. M.; Girolami, G. S. *J. Am. Chem. Soc.* **1999**, *121*, 5593. Hatlevik, Ø.; Buschmann, W. E.; Zhang, J.; Manson, J. L.; Miller, J. S. *Adv. Mater.* **1999**, *11*, 914.

(2) Sato, O.; Iyoda, T.; Fujishima, A.; Hashimoto, K. *Science* **1996**, *272*, 704. Ohkoshi, S.; Yorozu, S.; Sato, O.; Iyoda, T.; Fujishima, A.; Hashimoto, K. *Appl. Phys. Lett.* **1997**, *70*, 1040.

(3) Choi, H. J.; Sokol, J. J.; Long, J. R. *J. Phys. Chem. Solids* **2004**, *65*, 839. Zhong, Z. J.; Seino, H.; Mizobe, Y.; Hidai, M.; Fujishima, A.; Ohkoshi, S.; Hashimoto, K. *J. Am. Chem. Soc.* **2000**, *122*, 2952. Larionova, J.; Mathias, G.; Pilkington, M.; Andres, H.; Stoeckli-Evans, H.; Güdel, H. U.; Decurtins, S. *Angew. Chem., Int. Ed.* **2000**, *39*, 1605. Scuiller, A.; Mallah, T.; Verdaguer, M.; Nivorozkhin, A.; Tholence, J. L.; Veillet, P. *New J. Chem.* **1996**, *20*, 1.

(4) Sokol, J. J.; Hee, A. G.; Long, J. R. *J. Am. Chem. Soc.* **2002**, *124*, 7656. Berlinguette, C. P.; Vaughn, D.; Canada-Vilalta, C.; Galan-Mascaros, J. R.; Dunbar, K. R. *Angew. Chem., Int. Ed.* **2003**, *42*, 1523. Choi, H. J.; Sokol, J. J.; Long, J. R. *Inorg. Chem.* **2004**, *43*, 1606.

(5) Larionova, J.; Clérac, R.; Sanchiz, J.; Kahn, O.; Golhen, S.; Ouahab, L. *J. Am. Chem. Soc.* **1998**, *120*, 13088.

(6) Larionova, J.; Kahn, O.; Golhen, S.; Ouahab, L.; Clérac, R. *Inorg. Chem.* **1999**, *38*, 3621.

(7) (a) Larionova, J.; Kahn, O.; Golhen, S.; Ouahab, L.; Clérac, R. *J. Am. Chem. Soc.* **1999**, *121*, 3349. Note that the correct structure has been recently reported in: (b) Le Goff, X. F.; Clérac, R.; Coulon C.; Donnadieu, B. *J. Phys. IV* **2004**, *114*, 633.

(8) Stride, J. A.; Gillon, B.; Goukassov, A.; Larionova, J.; Clérac, R.; Kahn, O. *C. R. Acad. Sci., Ser. IIc: Chim.* **2001**, *4*, 105.

(9) Larionova, J.; Clérac, R.; Donnadieu, B.; Guérin, C. *Chem. Eur. J.* **2002**, *8*, 2712.

(10) Tanase, S.; Tuna, F.; Guionneau, P.; Maris, T.; Rombaut, G.; Mathonière, C.; Andruh, M.; Kahn, O.; Sutter, J. P. *Inorg. Chem.* **2003**, *42*, 1625.

(11) (a) Young, R. C. *J. Am. Chem. Soc.* **1932**, *54*, 1402. (b) Rossman, G. R.; Tsay, F. D.; Gray, H. B. *Inorg. Chem.* **1973**, *12*, 824. (c) Hursthouse, M. B.; Malik, K. M. A.; Soares, A. M.; Gibson, J. F.; Griffith, W. P. *Inorg. Chim. Acta* **1980**, *45*, L81.

(12) Compound **1** was obtained by slow diffusion in an H-shaped tube under argon of two deoxygenated 10^{-4} M aqueous solutions containing $K_4[Mo(CN)_7] \cdot 2H_2O$[11] and $[Mn(H_2O)_6](NO_3)_2 \cdot 6H_2O$, respectively, in the presence of $(NH_4)NO_3$ (10^{-4} M). After a few weeks, dark green crystals with an elongated plate shape formed. IR (Kbr, cm^{-1}): 2137 (w), 2106 (sh), 2086 (s), 2072 (sh), 1620 (s), 1410 (s).

10.1021/ic049513n CCC: $27.50 © 2004 American Chemical Society
Published on Web 07/07/2004

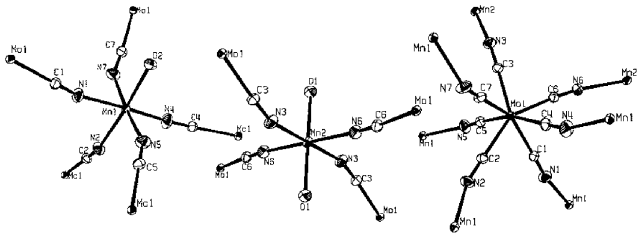

Figure 1. ORTEP drawings of local coordination environments of Mn1, Mn2, and Mo1 sites.

dimensional polymeric structure including $[Mo(CN)_7]^{4-}$, Mn^{2+}, $[NH_4]^+$, and water molecules coordinated to Mn ions or located in the void space of the structure.[13] Coordination spheres of the molybdenum and the two manganese, Mn1 and Mn2, sites are shown in Figure 1. Mo1 is surrounded by five N−C−Mn1 and two N−C−Mn2 linkages. The Mo−C bond lengths range from 2.120(2) to 2.165(2) Å, with a mean value of 2.139(2) Å. All of the Mo−C−N bond angles are relatively close to 180°; they range from 174.2(2)° to 179.1(2)°. Among the large number of possible polyhedra with seven vertices,[14] Mo1 adopts a distorted capped-trigonal prism geometry (Figure 1) also observed in most of the $[Mo(CN)_7]^{4-}/Mn^{2+}$ related compounds.[15] Mn1 and Mn2 atoms are, respectively, surrounded by five and four N−C−Mo linkages. In both cases, water molecules complete their octahedral coordination sphere (Figure 1). Mn−N and Mn−O bond lengths range from 2.162(2) to 2.262(2) Å, and from 2.240(2) to 2.271(2) Å, respectively. Mn−N−C bond angles deviate significantly from 180°; they range from 141.6(2)° to 166.4(2)°. The three-dimensional organization is based on a parallel arrangement of gridlike sheets similar to those observed for $K_2Mn_3(H_2O)_6[Mo(CN)_7]_2 \cdot 6H_2O$ (**2**). These layers are built from edge sharing $[Mo1-Mn1]_2$ lozenges and are arranged perpendicular to the *a** axis (Figure 2a). Mo1−Mn1 separation within this plane ranges from 5.275(2) to 5.461(2) Å. Moreover, Mo1/Mn1 layers are two by two linked (Figure 2b). Mo1 atoms of each

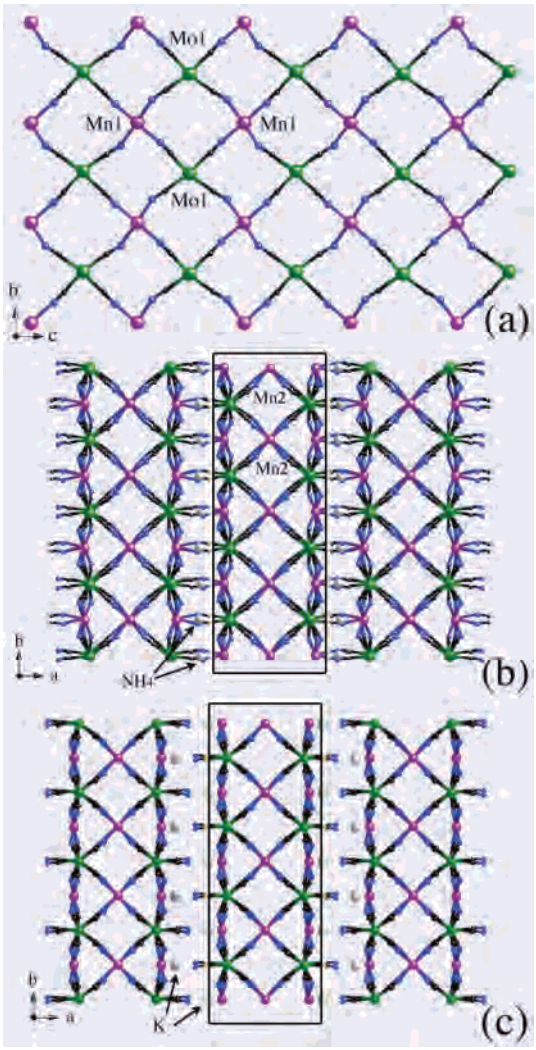

Figure 2. (a) View of the Mo1−Mn1 diamond-shaped layer in the *bc* plane in **1**. (b) Global view of the crystal structure of **1** emphasizing the repeating bilayer motif. (c) For comparison, a global view of the crystal structure for **2** from ref 7b. Hydrogen atoms and water molecules have been omitted for clarity.

plane are connected through $(NC)_2-Mn2-(CN)_2$ bridges to form bilayers reminiscent of the two-dimensional structure of **2** (Figure 2c). While in **2** these bilayers are well separated by K^+ and interstitial water molecules, they are connected together in **1** by direct Mo1−CN−Mn1 bridges to form the three-dimensional structure (Figure 2). Although the size of K^+ and $[NH_4]^+$ cations is similar (ca. 1.4 Å), the final crystal structure and its dimensionality are strongly influenced by their ability to interact and accommodate the network. This key point is well illustrated in **2** where the K^+ affinity for water molecules leads to an $(H_2O)K^+$ cation complex. While $(H_2O)K^+$ cations are too large and stabilized only a two-dimensional arrangement, $[NH_4]^+$ has the right size to accommodate the cubic cavity leading to the three-dimensional network in **1** (Figure 3).

Magnetic measurements[16] have been performed on polycrystalline samples of **1**. At high temperature, the $1/\chi$ versus *T* plot exhibits a nonlinear variation (Figure 4) as expected for ferrimagnetic behavior and observed in this family of compounds.[5−10] Below 53 K, *M*/*H* undergoes an abrupt

(13) Crystallographic data for **1**: C7H12N8O4Mn1.5Mo, MW = 450.59, monoclinic, *C*2/*c*, a = 29.025(6) Å, b = 7.1860(14) Å, c = 15.743(3) Å, β = 105.92(3)°, V = 3157.6(11) Å^3, Z = 8, T = 150(2) K, ρ = 1.896 g·cm^{-3}, λ(Mo Kα) = 0.71073 Å, Nonius Kappa CCD diffractometer, F(000) = 1772, μ = 2.003 mm^{-1}, 12705 reflections collected, 6906 of which were unique (R_{int} = 0.0216). DENZO-SMN was used for data integration, and SCALEPACK corrected data for Lorentz-polarization effects (Otwinowski Z.; Minor, W. *Methods Enzymol.* **1996**, *276*, 307). The structure was solved by direct methods and refined by a full-matrix least-squares method on F^2 using SHELXTL crystallographic software package (Sheldrick, G. M. *SHELXL97*, *Program for Crystal Structure Refinement*, and *SHELXS97*, *Program for Crystal Structure Solution*; University of Göttingen: Göttingen, Germany, 1997). All non-hydrogen atoms were refined anisotropically. The final refinement gave R = 0.0315 [$I > 2\sigma(I)$, 5850 reflections], *wR2* = 0.0852 [all data; 6906 reflections], GOF = 1.079 with 232 parameters. Additional crystallographic details are available as Supporting Information or by application to the Cambridge Crystallographic Data Centre (CCDC 235836), 12 Union Road, Cambridge CB21EZ, U.K. (Fax: (+44) 1223-336-033. E-mail: deposit@ccdc.cam.ac.uk.)

(14) Muetterties, E. L.; Wright, C. M. *Q. Rev., Chem. Soc.* **1967**, *21*, 109.

(15) For the $[Mo(CN)_7]^{4-}$ unit, two geometries have been observed: the capped trigonal prismatic (CTP-C_{2v}) in $Mn_2(tea)Mo(CN)_7 \cdot H_2O$,[10] $[N(CH_3)_4]_2Mn_3(H_2O)_3[Mo(CN)_7]_2 \cdot 2H_2O$,[9] $K_4[Mo(CN)_7]$,[11b] $Mn_2(H_2O)_5Mo(CN)_7 \cdot 4.75H_2O$,[6] and $K_2Mn_3(H_2O)_6[Mo(CN)_7]_2 \cdot 6H_2O$,[7] and pentagonal bipyramid (PBP-D_{5h}) in $NaK_3[Mo(CN)_7]$[11c] and $Mn_2(H_2O)_5Mo(CN)_7 \cdot 4H_2O$.[5]

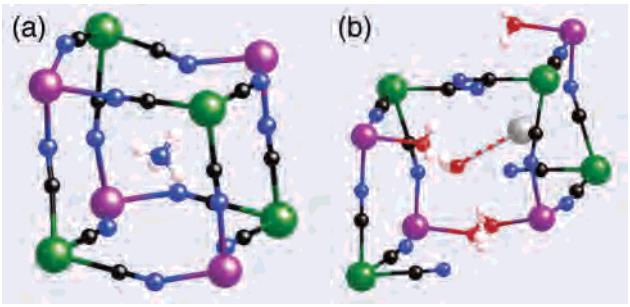

Figure 3. View of the countercation accommodation in (a) **1** and (b) **2** emphasizing its key role on the final dimensionality of the material.

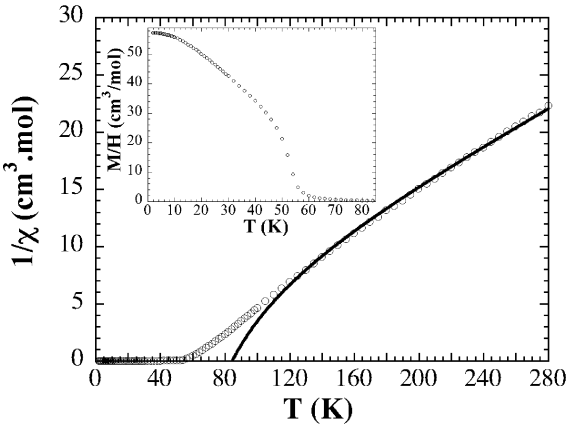

Figure 4. Temperature dependence of $1/\chi$ (where χ is defined as M/H) at 1 kOe for **1** above 53 K fitted to the model described in the text (solid line). Inset: temperature dependence of M/H at 1 kOe.

increase suggesting the onset of a magnetic ordering (inset Figure 4). As expected for a magnet, the first magnetization at 1.8 K increases rapidly from 0 to 11.5 μ_B below 2 kOe, and then slowly reaches 13.3 μ_B at 50 kOe (Figure 5). Note that no significant hysteresis effect on the magnetization has been observed down to 1.8 K. At high fields, M is close to the saturation value of 13 μ_B expected for antiferromagnetic $Mn^{II}-Mo^{III}$ interactions. This interaction, J_{Mo-Mn}, can be estimated by modeling the high-temperature magnetic susceptibility using a mean-field ferrimagnetic model.[17] Above 110 K, far from the transition (i.e., where the mean-field approximation is still valid), $1/\chi$ can be well reproduced with $g = 1.96$[18] and $J_{Mo-Mn}/k_B = -8.7$ K (Figure 4). The negative

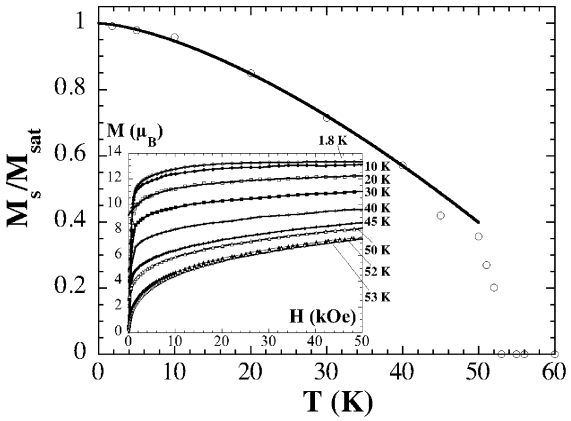

Figure 5. Temperature dependence of the spontaneous magnetization, M_s, normalized at the saturation value, M_{sat}, obtained at 1.8 K for **1**. Solid line represents the $T^{3/2}$ Bloch law discussed in the text. Inset: Field dependence of the magnetization at temperatures ranging from 1.8 to 53 K.

sign of J_{Mo-Mn} confirms the dominating antiferromagnetic interactions and the ferrimagnetic nature of **1**. It is worth noticing that J_{Mo-Mn} obtained here is in agreement with values reported for $Mn_2(H_2O)_5[Mo(CN)_7]\cdot 4H_2O$[5] (−4.5 K) and $Mn_2(tea)[Mo(CN)_7]\cdot nH_2O$ (where tea is triethanolamine)[10] (−6 and −9 K). Removing the demagnetizing factor (N) dominating at low field,[19] the spontaneous magnetization (M_s) can be deduced from M versus H curves at different temperatures (inset Figure 5).[5] When the temperature is increased, M_s vanishes at the critical temperature, 53 K. The thermal variation of M_s is directly related to the lowest branch of the magnon spectra for which the frequency is proportional to the square of the wave vector in the ferrimagnetic case.[20] At low temperature, this theoretical result leads to a temperature dependence of M_s/M_{sat} in $T^{3/2}$ (Bloch law).[20] As shown in Figure 5, experimental results agree perfectly with this prediction and definitively confirm the stabilization of a ferrimagnetic ordered state at 53 K.

In conclusion, **1** illustrates how the choice of the counterion can be crucial to control the dimensionality of a material and its magnetic properties. Replacing the $[(H_2O)K]^+$ cation by $[NH_4]^+$ allows the cyano-based $Mo^{III}-Mn^{II}$ network to become three-dimensional and allows a significant enhancement of the ferrimagnetic transition from 39 to 53 K.

Acknowledgment. The authors would like to thank the CNRS, the Université Bordeaux 1, and the Conseil Regional d'Aquitaine for financial support. We are also grateful to Dr. Yang-Guang Li for his help in the structure analysis.

Supporting Information Available: X-ray crystallography experimental details (CIF format). This material is available free of charge via the Internet at http://pubs.acs.org.

IC049513N

(16) A Quantum Design SQUID MPMS-XL susceptometer has been used to perform magnetic susceptibility measurements on four different polycrystalline samples of **1** (4.15, 4.10, 4.78, 7.80 mg) in the temperature range 1.8−300 K, with fields up to 5 T. The magnetic data were corrected for the sample holder, and the diamagnetic contribution was calculated from Pascal's constants (Boudreaux, E. A.; Mulay, L. N. *Theory and Applications of Molecular Paramagnetism*; John Wiley Sons: New York, 1976).

(17) Kittel, C. *Introduction to Solid State Physics*; Wiley: New York, 1996; p 461. Note that this model has been generalized in the case of 2 Mo^{III} and 3 Mn^{II} per unit cell taking into account that Mn−Mo magnetic interactions are all identical. Therefore, the reported J_{Mo-Mn} is an average value defined by the following Hamiltonian: $H = -2J_{Mo-Mn}\sum_{\langle i,j\rangle}S_{Mo,i}S_{Mn,j}$, where the sum is extended over all Mo and Mn pairs.

(18) The g value is slightly low due to some extrinsic diamagnetic impurities always present in the different batches measured.

(19) The obtained N value is 4.5, which is very close to the expected one for a spherical crystal, $4\pi/3$. (See for example: Herpin, A. *Théorie du Magnétisme*; Presses Universitaires de France: Paris, 1968; p 25.)

(20) Madelung, O. *Introduction to Solid State Theory*; Springer-Verlag: Berlin, 1978, p 163.